Theoretical Investigation on the Dissociation of (R)-Benzoin Catalyzed by Benzaldehyde Lyase

Jing Zhang,[a,b] Xiang Sheng,[c] QianQian Hou,[c] and Yongjun Liu*[a,c]

Benzaldehyde lyase (BAL) is a versatile thiamin diphosphate (THDP)-dependent enzyme with widespread synthetic applications in industry. Besides lyase activity, BAL also performs the functions as carboligase and decarboxylase. Unlike many other THDP-dependent enzymes, the active center of BAL is devoid of any acid-base amino acid residues except Glu50 and His29, and therefore, the catalytic mechanism of BAL is unusual. In this article, the dissociation mechanism of (R)-benzoin to benzaldehyde catalyzed by BAL has been studied by using density functional theory method. The calculation results indicate that the whole reaction consists of four elementary steps, and at least two steps contribute to rate-limiting. A big difference with other THDP-dependent enzymes is that, in the first stage of the reaction, the ligation of substrate and THDP ylide is not companied by proton transfer, and in the subsequent transition states and intermediates, the carbonyl oxygen always exists in the form of anion. Gln113, His29, and 4′-amino group of THDP are found to have the function to stabilize the transition states and intermediates. His29 acts as the proton acceptor in step 2 and proton donor in step 3 using one water molecule as mediator. © 2013 Wiley Periodicals, Inc.

DOI: 10.1002/qua.24573

Introduction

Lyases are a class of enzymes that catalyze the cleavage of C—C, C—O, C—N, and other bonds by other means than by hydrolysis or oxidation, which have aroused great interest in the food and cosmetic industries owing to their application as biocatalysts.[1,2] Benzaldehyde lyase (BAL, EC 4.1.2.38) is a thiamin diphosphate (THDP)-dependent enzyme, which catalyzes the reversible conversion of aromatic 2-hydroxy ketones like (R)-benzoin to benzaldehyde, as shown in Scheme 1.[3] The ability of BAL to cleave acyloin linkages with strict R-selectivity, which can be used in the kinetic resolution of racemic benzoins, has not yet been observed in other enzymes.[4] Besides catalyzes the dissociation reaction, BAL also acts as a carboligase and catalyzes the carboligation of two aldehydes with high stereo- and substrate specificity.[5] This is of utmost synthetic interest especially the ability to catalyze the formation of chiral α-hydroxy ketones as they are important building blocks for various pharmacologically active compounds.[6,7] Recently, BAL is also testified to have the weak activity of decarboxylase which can catalyze the decarboxylation of benzoylformate to form benzaldehyde and (R)-benzoin.[8] Furthermore, it bears the ability to catalyze the C—N bond formation with aromatic aldehydes and nitrosobenzene derivatives as substrates to obtain N-arylhydroxamic acids.[9] This broad range of reactions makes BAL unique among the well-characterized THDP-dependent enzymes.[10]

Up to now, several high-resolution X-ray data have provided deep insight into the structures of BAL.[3,11,12] For example, Maraite et al.[3] reported the high resolution (1.65 Å) crystal structure of BAL from *Pseudomonas fluorescens* (PDB code: 2UZ1). In general, the enzyme is a homotetramer of 4 × 563 amino acid residues with a molecular mass of 58,919 Da/monomer. The four subunits A, B, C, and D are grouped to form two tight dimers namely A-B and C-D. Each subunit consists of three domains, that is, Dom-α, Dom-β, and Dom-γ, and each of them binds one THDP cofactor using one Mg^{2+} as a scaffold for the diphosphate moiety. The THDP cofactor is bound in a deep pocket which is connected with the exterior of the protein by a channel containing water molecules. Residues from Dom-γ make interactions with the diphosphate moiety of THDP and magnesium, whereas those from Dom-α of a neighboring subunit bind to the pyrimidine ring of THDP. From the active center of *Pseudomonas fluorescens* BAL (shown in Fig. 1a), we can see that this enzyme shares some similarities with most other THDP enzymes.[13–18] First, a glutamate residue (Glu50) is located within hydrogen bonding distance from N1′ of THDP. Second, the coenzyme THDP adopts the so-called V-conformation to bring the N4′-amino group of the pyrimidine ring adjacent to the C2 of the thiazolium ring, greatly facilitating the formation of ylide to initiate the catalytic cycle. A major difference between BAL and many other THDP-dependent enzymes, such as pyruvate decarboxylase (PDC) and transketolase (TK), lies in the fact that the active

[a] *J. Zhang and Y. Liu*
Northwest Institute of Plateau Biology, Chinese Academy of Sciences, Xining, Qinghai 810001, China
Fax: (+86) 531 885 644 64
E-mail: yongjunliu_1@sdu.edu.cn
[b] *J. Zhang*
Key Laboratory of Inorganic Chemistry in Universities of Shandong (Jining University), Qufu, Shandong 273155, China
[c] *X. Sheng, Q. Hou and Y. Liu*
School of Chemistry and Chemical Engineering, Shandong University, Jinan, Shandong 250100, China

Contract grant sponsor: Natural Science Foundation of China; contract grant number: 21173129, 21373125.

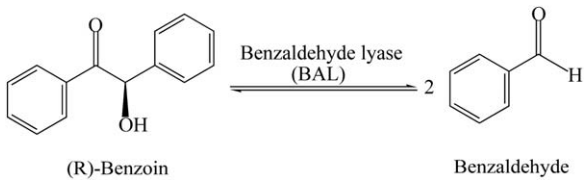

Scheme 1. The dissociation of (R)-benzoin catalyzed by BAL.

center of BAL is devoid of any acid-base amino acid residues except Glu50 and His29.[8,15,17]

A possible mechanism for the reversible dissociation of benzoin has been proposed, as shown in Scheme 2.[11] Similar with other THDP-dependent enzymes, the catalytic cycle also starts with the nucleophilic attack of THDP ylide at the carbonyl carbon of (R)-benzoin, producing the first covalent intermediate C2-(α,β-dihydroxy-α,β-diphenyl)-ethyl THDP (DDETHDP) (step 1). Then, the first benzaldehyde is released from DDETHDP, and the carbanion/enamine intermediate is formed (step 2). In the third step (step 3), the carbanion/enamine intermediate abstracts a proton from the neighboring residue to form C2α-hydroxybenzyl THDP (HBTHDP). In the final step (step 4), the second benzaldehyde is released and the THDP ylide is regenerated. In the past years, numerous experimental studies have paid more attention to the synthetic capability of BAL,[19–24] but relatively little researches were focused on the catalytic mechanism of BAL.[8,11] In a stopped-flow photodiode array (PDA) experiment in which BAL was mixed with (R)-benzoin, a weak absorption with λ_{max} of 393 nm was observed, which implied that the reaction may undergo the enamine intermediate. Additional circular dichroism and PDA experiments on the reaction between BAL and (E)-3-(pyridine-3-yl) acrylaldehyde (PAA) also confirmed the formation of covalent THDP-bound intermediate, which was actually an analog of HBTHDP.[8]

The active center of BAL, either the enzyme with bound cofactor THDP (PDB code: 2UZ1) or the enzyme in its covalent complex with methyl benzoylphosphonate (PDB code: 3D7K), reveals that only Glu50 and His29 are possible proton donor/acceptor.[3,11,12] Glu50 is a universally conserved residue in most of THDP-dependent enzymes, which is presumed to participate in the acid-base chemistry leading to the formation of 1′, 4′-iminopyrimidine tautomer.[8,11] His29 is hydrogen bonded to a water molecule which is 3.6 Å far from the C2 of THDP.[3] When His29 was substituted with alanine, the measured activity in the presence of 0.50 mM THDP was only 2.7% (H29A) compared to the activity of wild-type BAL.[11] Modeling of R-benzoin or DDETHDP into the active center of BAL suggested that the side chain of His29 may play a role in deprotonating the "distal" OH group of bound benzoin, leading to the release of the first benzaldehyde molecule thereby forming the enamine intermediate. The remaining activated aldehyde is then protonated and released. The protonation is probably performed by the water attached to His29.[11,12]

As outlined above, incomplete studies about the reaction mechanism of BAL have been conducted, and open questions still remain. For example, as the active center of BAL is lack of acid-base amino acid residues, how the only candidate His29 plays its role in the proton transfer during the catalytic cycle? Whether His29 offers a proton first to benzoin to release DDETHDP, and then abstracts the proton back from DDETHDP to form enamine? Moreover, the role of the water molecule attached to His29, the detailed description of each elementary step, the roles of other pocket residues involved in proton transfer, and stabilization of reaction intermediates and transition states, are still not fully understood. In this article, we present a theoretical study on the mechanism of (R)-benzoin dissociation catalyzed by BAL using hybrid density functional theory (DFT) method on a cluster model, which has been testified to be successful in studying enzyme active sites and reaction mechanisms.[25–29] A number of recent works about THDP-dependent enzymes have also given reasonable results by using this methodology. For example, Wang et al. explored all the elementary steps involved in the catalytic cycle of PDC.[30] The catalytic roles of residues in the active site of PDC

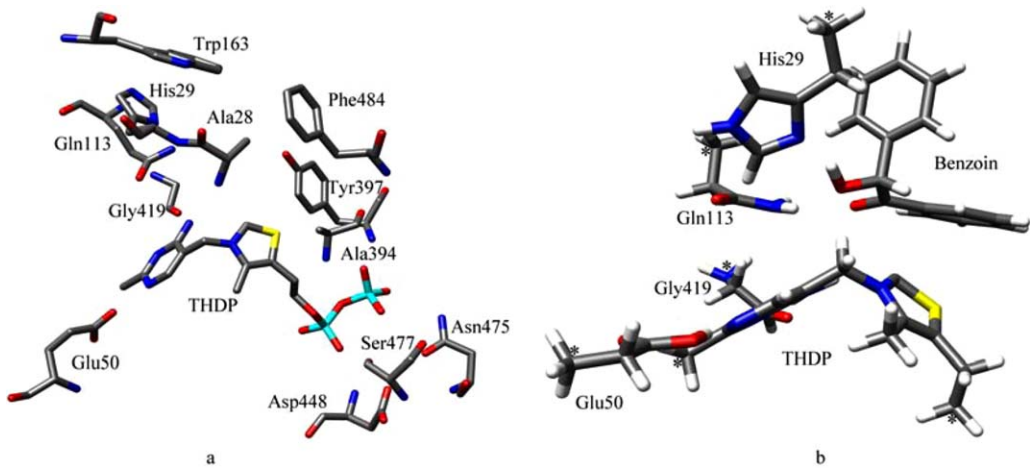

Figure 1. (a) The active site of BAL with the cofactor THDP (PDB code 2UZ1); (b) The calculation model used in the present work. The benzoin molecule is separately optimized and then deposited into the active pocket using the Autodock program. The fixed atoms are labeled by asterisks. [Color figure can be viewed in the online issue, which is available at wileyonlinelibrary.com.]

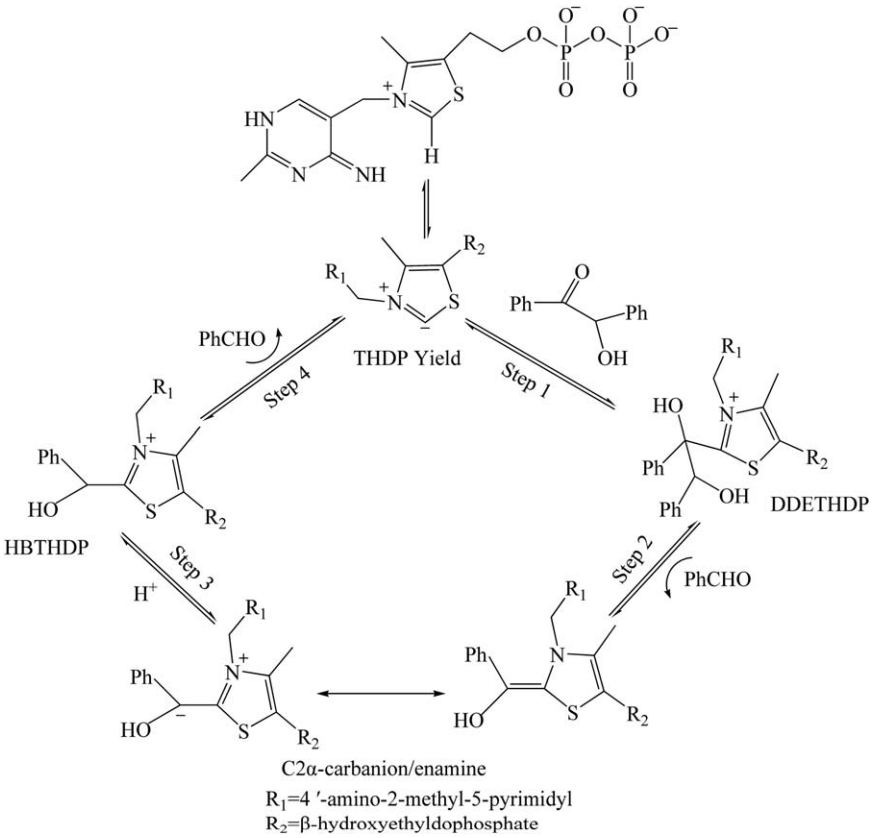

Scheme 2. Proposed catalytic mechanism of BAL for the reversible benzoin dissociation.

in individual steps elucidated from their study are in good agreement with those derived from site-directed mutagenesis. Sheng et al. studied the transfer mechanism of a 2-carbon fragment between a donor D-xylulose 5-phosphate and an acceptor D-ribose 5-phosphate catalyzed by TK,[31] which provides useful reaction details and clearly illustrates the reaction mechanism. It should be noted that the combined quantum mechanics and molecular mechanics (QM/MM) method is increasingly developed in recent years for investigating the fundamental and practical problems of enzymology.[32,33] But the available QM/MM methods are usually expensive. Our present aim is to qualitatively understand the transition state structures and energetics of the catalytic reaction. Therefore, for such a complex system, the DFT method with cluster models was selected.

Computational Details

In the present study, all calculations were performed by using hybrid DFT method implemented in Gaussian 09 program package.[34] Molecular geometries were optimized at B3LYP/6-31G(d,p) level of theory in gas phase. The benzoin molecule was separately optimized and then placed into the active site using the Autodock program.[35] Some truncated atoms were fixed to their crystallographic positions to prevent unrealistic movements of the groups during the optimization. To obtain more accurate energies, single-point calculations were performed with larger basis set 6-311++G(2d,2p) on the B3LYP/6-31G(d,p) optimized geometries. Frequencies were calculated at the B3LYP/6-31G(d,p) level to acquire zero-point vibrational energies (ZPE) and to ascertain that all the optimized geometries correspond to a local minima that has no imaginary frequency or a saddle point that has only one imaginary frequency. As some atoms were frozen during the optimization, a few small negative eigenvalues usually appear, typically in the order of 10–30 cm^{-1}. These frequencies do not contribute significantly to the zero-point energies and can be ignored. For each transition state, intrinsic reaction coordinate calculations were performed to guarantee its correct connection to the designated local minima. To evaluate the effects of solvation effect on the energetics of each elementary step, we also used the polarizable-continuum model (PCM)[36,37] to calculate the single-point energies at 6-311++G(2d,2p) level for each species on the optimized geometries. The dielectric constant of the enzyme environment in this model was chosen to be 4. This method is reliable and can dramatically reduce the computational expense which has been used in many previous studies.[38–40]

Results and Discussions

THDP ylide was chosen as the beginning form of THDP in our calculation model in view of the extensive researches about the activation mechanism of THDP had been made.[41–43] Experimental studies have proved that the universally conserved residue Glu50 and the only candidate of general acid-base catalyst His29 play important roles in the catalytic cycle. In addition, the imino group of THDP is hydrogen bonded to

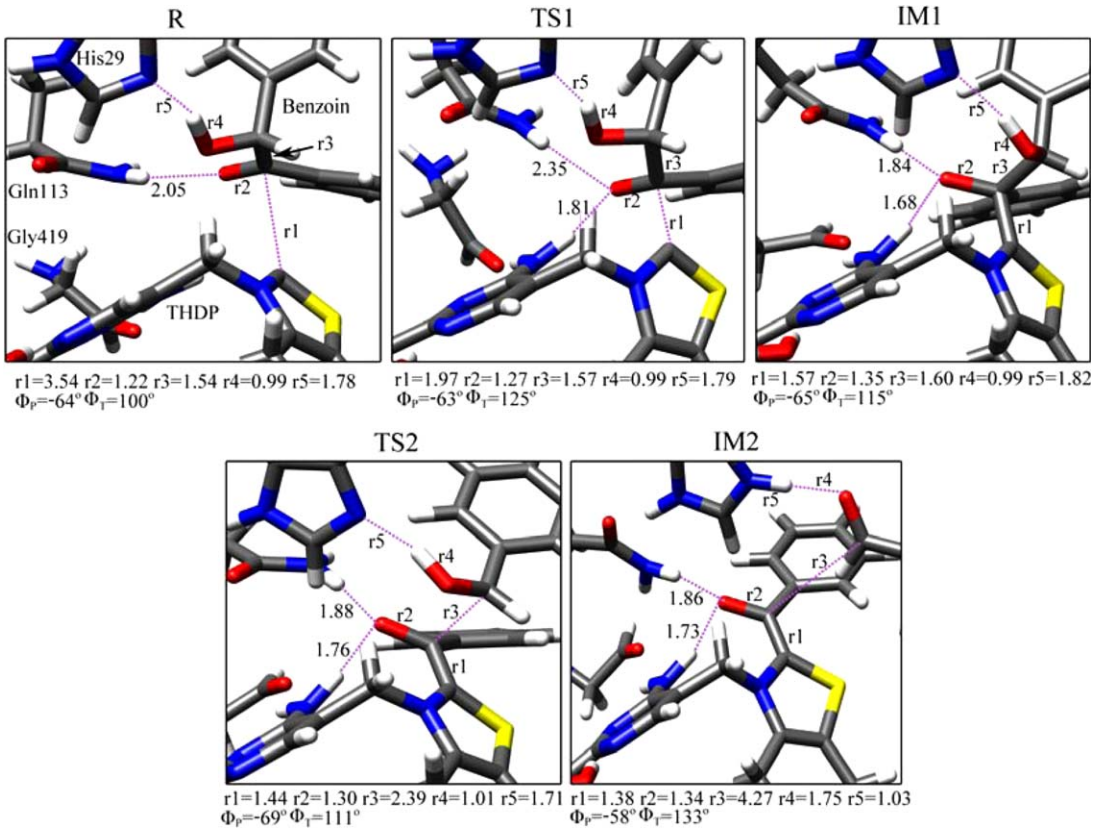

Figure 2. The truncated active center of the optimized geometries for various species in the first half-reaction obtained at the B3LYP/6-31G(d,p) level. The key bond distances are shown in angstrom and characteristic torsion angles Φ_T and Φ_P for the orientation of the THDP rings are shown in degree. [Color figure can be viewed in the online issue, which is available at wileyonlinelibrary.com.]

the carbonyl of Gly419, and Gln113 forms hydrogen bond interaction with the coming substrate benzoin.[11,12] Therefore, Glu50, His 29, Gly419, and Gln113 were included in the calculation model (shown in Fig. 1b). To decrease the computational consumption, the side chains of these residues were truncated, and the truncated atoms were fixed to their crystallographic positions during the optimization, which were marked with asterisks in Figure 1b. The V-conformation of the THDP enforced by the protein framework is important for its catalytic activity, therefore, the characteristic torsion angles Φ_T and Φ_P were usually frozen in some earlier studies.[30,44,45] We used different strategy to freeze the THDP ylide in which the terminal and truncated carbon atoms of THDP ylide were frozen. This strategy can also keep the V-conformation of the THDP, but the middle moiety of THDP is still flexible. The torsion angles Φ_T and Φ_P for defining the orientation of THDP rings in all species will be given in the corresponding figures.

To facilitate a clear elucidation of the catalytic cycle, the whole reaction was divided into two parts: the first half-reaction and the second half-reaction. They will be discussed in detail in the following sections.

First half-reaction

The first half-reaction begins with the reaction of THDP ylide and benzoin, and ends with the formation of C2α-carbanion/enamine (step 1 and step 2 in Scheme 2). According to the proposed mechanism, the two important intermediates DDETHDP and C2α-carbanion/enamine are simplified to IM1 and IM2 in our calculations. The optimized structures of initial reactant (R), transition states (TS1 and TS2), and intermediates (IM1 and IM2) are shown in Figure 2.

From Figure 2, we can see that in reactant (R) the substrate R-benzoin is stabilized by two hydrogen bonds from His29 and Gln113. The hydrogen bond length (*r*5) between His29 and the hydroxyl group of benzoin is very short (1.78 Å) while that of Gln113 with the carbonyl group of benzoin is relatively long (2.05 Å). The reactive C2 atom of thiazolium ring of THDP positions a distance (*r*1) of 3.54 Å from the carbonyl carbon atom (Cα) of benzoin and defines the angle of 106° with the Cα and O atoms. This optimized structure offers admirable facilities for the nucleophilic attack of C2 atom of the thiazolium ring to the Cα of benzoin under the expected Bürgi–Dunitz angle of 103° ± 3°.[46] In transition state TS1, the distance of C2—Cα (*r*1) changes from 3.54 to 1.97 Å and the distance of hydrogen atom of 4′-amino group with the carbonyl oxygen atom changes to 1.81 Å from 3.40 Å. In IM1, the C2—Cα bond is formed with a distance of 1.57 Å (*r*1), but the proton transfer to the carbonyl oxygen does not occur at this stage. This is different with other THDP-dependent enzymes that the formation of C2—Cα bond is accompanied by a proton transfer.[30,33] The quondam carbonyl oxygen still exists in the form of oxygen anion, which is stabilized by two hydrogen bonds from the 4′-amino group of THDP and Gln113. The

hydrogen bond lengths between the oxygen anion and the hydrogen atom of 4′-amino group or Gln113 are 1.68 and 1.84 Å, respectively. In addition, the hydrogen bond length (*r*5) between His29 and the hydroxyl group of benzoin is 1.82 Å, which will favor the next proton transfer.

As shown in Scheme 2 and Figure 2, the next step is the cleavage of C—C carbon bond (*r*3) of benzoin to release the first benzaldehyde and generate C2α-carbanion/enamine intermediate IM2 via TS2. In TS2, the C—C distance (*r*3) changes from 1.60 to 2.39 Å, but the proton transfer from the hydroxyl group of benzoin to His29 does not start yet. In IM2, the C—C carbon bond (*r*3) further elongated from 2.39 to 4.27 Å, which means the C—C bond has completely broken. At the same time, the proton of the hydroxyl group of benzoin transfers to His29, and *r*5 changes from 1.71 to 1.03 Å. By comparing the structures of IM1, TS2, and IM2, we can see that the cleavage of C—C bond and the proton transfer from the hydroxyl group of benzoin to His 29 take place in a concerted manner but not precisely synchronous. The beginning of proton transfer is much later than the cleavage of C—C bond. During this step, the two hydrogen bonds between the oxygen anion and the hydrogen atom of 4′-amino group or Gln113 are still kept, and the oxygen anion still exists, that is, the hydroxy connected with C2α in C2α-carbanion/enamine exists in the form of oxygen anion. Moreover, C2—C2α carbon bond (*r*1) changes from single bond to double bond during this step, and the geometry of C2α-carbanion/enamine is planar but not pyramidal. This geometry agrees well with the experimental results detected by electronic spectroscopy on the enzyme from a true substrate benzoin that the enamine intermediate is planar and highly conjugated.[8]

The energy profile in gas phase is shown in Figure 4. We can see that the energy barriers for the formation of IM1 and IM2 are 13.21 and 11.81 kcal/mol, respectively, implying that both of the two steps are easy to occur. In addition, the relative energy of IM2 is 4.15 kcal/mol lower than that of the reactant (R), meaning the first-half reaction is favorable, and the intermediate IM2 is relatively stable, which is in good agreement with the experimental observation of Chakraborty.[8] In the stopped-flow PDA experiment mixing BAL with (R)-benzoin, the enamine intermediate (IM2) was observed with λ_{max} at 393 nm, which was stable for 2 min with a rate of intermediate formation of 0.031 s^{-1}.[8]

Second half-reaction

In all crystal structures of BAL, a water molecule was identified at a distance of about 3.6 Å from the C2 atom of THDP.[3,11,12] This water molecule forms hydrogen bonds with Gln113 and His29. When the substrate R-benzoin was docked into the active center, the hydroxyl of benzoin occupies the position of water molecule.[12] We consider that, after the releasing of first benzaldehyde, this water molecule may come back again to participate in the second half-reaction. Therefore, we studied two reaction pathways, that is, pathway 1 without water molecule and pathway 2 assisted with a water molecule.

Pathway 1. The second half-reaction starts with the attack of a hydrogen atom on the C2α of C2α-carbanion/enamine to generate HBTHDP, which then releases the second benzaldehyde (step 3 and step 4 in Scheme 2) to complete the catalytic cycle.

After the first benzaldehyde was removed from IM2, IM3 was obtained, as shown in Figure 3. From IM3, we can see that, the only possible hydrogen donor is the 4′-amino group of THDP, and the distance between the hydrogen of 4′-amino group and the C2α of C2α-carbanion/enamine (*r*3) is 2.27 Å, which is favorable for proton transfer. In transition state TS3, *r*3 changes to 1.27 Å from 2.27 Å, and *r*4 changes to 1.49 Å from 1.01 Å. In the meantime, the planar C2α-carbanion/enamine evolves to the tetrahedral configuration due to the change of hybridization of C2α from sp^2 to sp^3. In IM4, the hydrogen atom has been transferred to the C2α of C2α-carbanion/enamine, meaning the formation of C2α-oxygen anion benzyl THDP rather than C2α-HBTHDP. Oxygen anion is stabilized by two hydrogen bonds from His29 and Gln113.

The last step of the catalytic cycle is the release of the second benzaldehyde which requires the cleavage of C2—C2α bond. TS4 in Figure 3 shows that C2—C2α bond length (*r*1) changes from 1.54 to 2.34 Å, and the distance (*r*2) between C2α and oxygen anion changes from 1.37 to 1.25 Å, forming the carbonyl again. From the structure of *P*, we can see that benzaldehyde breaks from the cofactor, and the THDP ylide is regenerated.

Figure 4 shows that the energy barriers for the formation of IM4 and *P* are 24.44 and 12.77 kcal/mol, respectively, suggesting the formation of IM4 to be the rate-determining step. But, all the relative energies of IM4 and *P* are higher than that of IM3, indicating the energy requirement of the second half-reaction is high. It is definitely not favorable in energy.

Pathway 2. In this pathway, the first benzaldehyde was replaced by a water molecule, and IM3′ was obtained after optimization, as shown in Figure 5. From IM3′, we can see that the water molecule forms a hydrogen bond with His29 with a distance of 1.80 Å (*r*5). Besides, the distance (*r*3) between the C2α of C2α-carbanion/enamine and the hydrogen of water molecule is 2.65 Å, which is in favor of proton transfer.

Structure of transition state TS3′ indicates the water molecule to be an ideal medium for the proton transfer from His29 to the C2α of C2α-carbanion/enamine, that is, the hydrogen transfer from the water molecule to the C2α of C2α-carbanion/enamine and the hydrogen transfer from His29 to the oxygen atom of the water molecule proceed in a concerted manner. Similar with pathway 1, from TS3′ to IM4′, the hybridization of C2α changes from sp^2 to sp^3, and the planar C2α-carbanion/enamine changes to tetrahedral configuration. In IM4′, C2α-oxygen anion still exits, which is stabilized by two hydrogen bonds from 4′-amino group and Gln113.

The next step is the cleavage of C2—C2α bond to release the second benzaldehyde. As shown in TS4′, C2—C2α bond length (*r*1) changes to 2.28 Å from 1.55 Å, and the distance (*r*2) between the C2α and oxygen anion changes to 1.26 Å from 1.36 Å, which indicates the formation of carbonyl again.

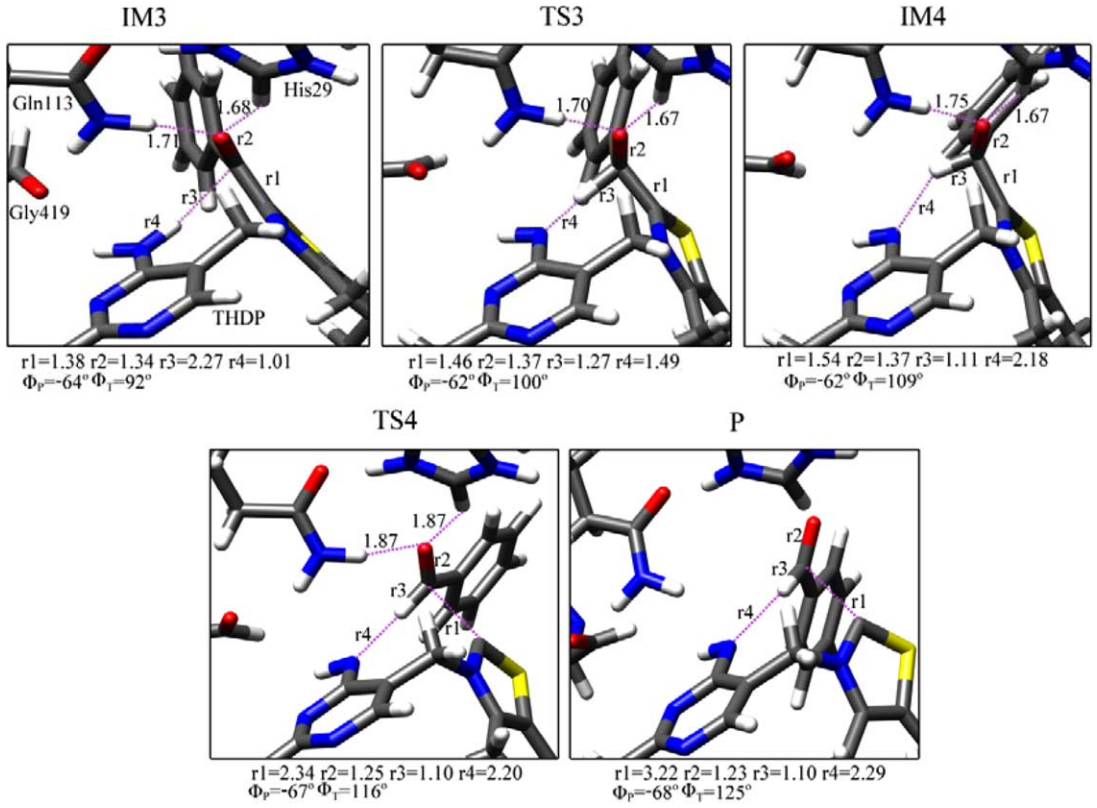

Figure 3. The truncated active center of the optimized geometries for various species in the second half-reaction obtained at the B3LYP/6-31G(d,p) level (pathway 1). The key bond distances are shown in angstrom and characteristic torsion angles Φ_T and Φ_P for the orientation of the THDP rings are shown in degree. [Color figure can be viewed in the online issue, which is available at wileyonlinelibrary.com.]

The second benzaldehyde breaks from THDP completely in P′ which proclaims the end of the whole catalytic cycle.

The energy profile of the whole reaction in which the second half-reaction proceeds via pathway 2 is shown in Figure 6. We can see that the energy barrier for the formation of C2α-oxygen anion-benzyl THDP (IM4′) is much lower than that of IM4 in Figure 4 (14.20 vs. 24.44 kcal/mol), and the relative energies of IM4′ and P′ are 7.15 and 4.56 kcal/mol lower than that of IM3′, respectively. The stability of IM4′ is consistent with the experimental observations.[8] A stable broad absorbance at λ_{max} = 456 nm was observed in the stopped-flow PDA studies of the reaction between BAL and PAA, which is assigned to the analog of HBTHDP (IM4′). The small energy barriers of pathway 2 indicate the important role of water molecule for the proton transfer from His29 to C2α-carbanion/enamine. With the assistance of water molecule, the rotation of His29 is no longer required for the proton transfer from His29 to C2α-carbanion/enamine. In addition, to evaluate the effect of protein environment on the energy barriers, single-point calculations at the level of 6-311++G(2d,2p) basis set

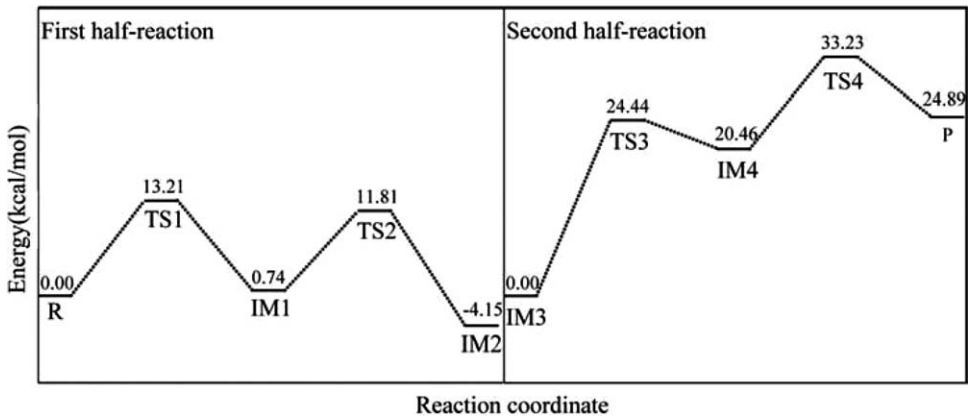

Figure 4. Energy profile for the whole BAL catalytic process in gas phase with the second half-reaction proceeds in pathway 1. The ZPE-corrected relative energies are obtained at the B3LYP/6-311++G(2d,2p)// B3LYP/6-31G(d,p) level.

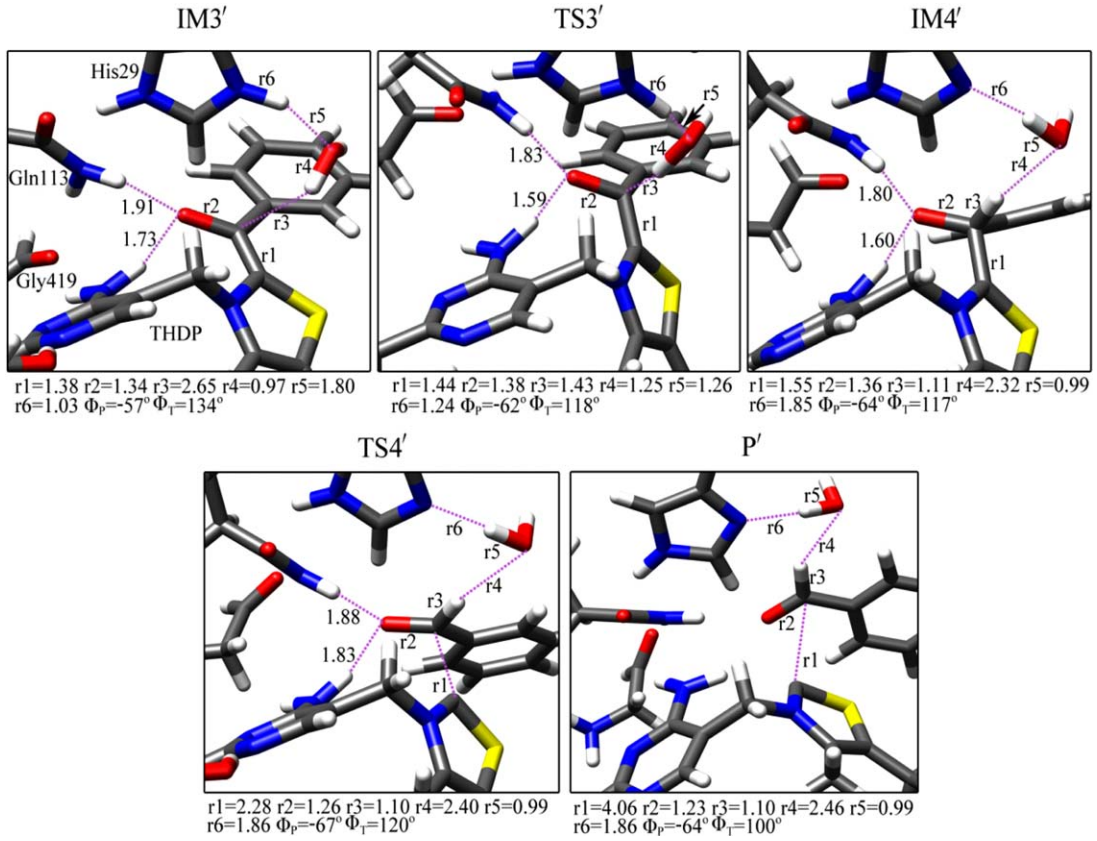

Figure 5. The truncated active center of the optimized geometries for various species in the second half-reaction obtained at the B3LYP/6-31G(d,p) level (pathway 2). The key bond distances are shown in angstrom and characteristic torsion angles Φ_T and Φ_P for the orientation of the THDP rings are shown in degree. [Color figure can be viewed in the online issue, which is available at wileyonlinelibrary.com.]

were also performed on the B3LYP/6-31G(d,p) optimized geometries by using the PCM. The calculation results are shown in Figure 6, which indicate that the enzyme environment exerts remarkable but different influences on each elementary step.

Conclusions

The detailed mechanism of the dissociation of (R)-benzoin to benzaldehyde catalyzed by BAL has been studied by using DFT method. The calculations indicate that the catalytic cycle consists of four elementary steps. Step 1 is the ligation of THDP ylide and substrate to form the first covalent intermediate C2-(α,β-dihydroxy-α,β-diphenyl)-ethyl THDP (DDETHDP), and step 2 involves the C—C bond cleavage of the substrate leading to the formation of carbanion/enamine intermediate and release of first benzaldehyde. Step 3 is a proton transfer process, in which the most possible proton donor His29 uses one water molecule as mediator. Step 4 corresponds to the split of intermediate C2α-hydroxybenzyl THDP (HBTHDP) to release the second benzaldehyde and regenerate THDP ylide. Gln113, His29, and 4′-amino group of THDP are found to have the function to stabilize the transition states and intermediates. His29 behaves as proton acceptor in step 2 and proton donor in step 3. By comparing the energy profile, we found that three elementary steps, step 1, step 2, and step 4, correspond to similar energy barriers of 14.30, 16.36, and 15.58

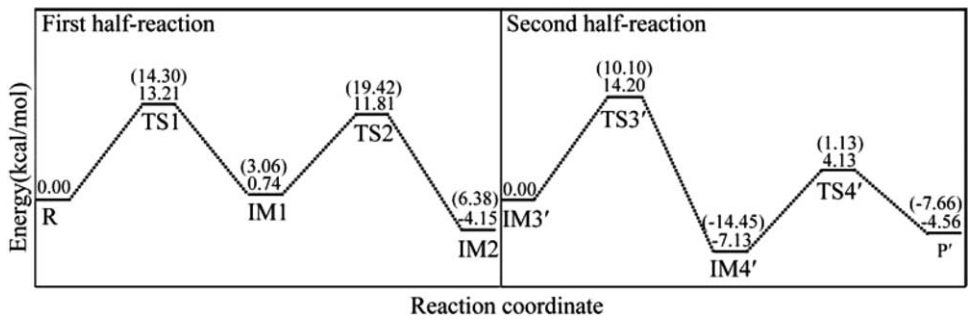

Figure 6. Energy profile for the whole BAL catalytic process in gas phase and in solution phase (values in brackets) with the second half-reaction proceeds in pathway 2. The ZPE-corrected relative energies are obtained at the B3LYP/6-311++G(2d,2p)// B3LYP/6-31G(d,p) level.

kcal/mol, respectively, suggesting all of them contribute to the overall rate. These results may provide useful information for understanding the catalytic reaction of BAL.

Keywords: benzaldehyde lyase · density functional theory method · reaction mechanism · THDP-dependent enzyme · R-benzoin

How to cite this article: J. Zhang, X. Sheng, Q. Hou, Y. Liu. *Int. J. Quantum Chem.* **2014**, *114*, 375–382. DOI: 10.1002/qua.24573

[1] G. Grogan, J. Graf, A. Jones, S. Parsons, N. J. Turner, S. L. Flitsch, *Angew. Chem. Int. Ed.* **2001**, *40*, 1111.
[2] P. M. Leonard, A. M. Brzozowski, A. Lebedev, C. M. Marshall, D. J. Smith, C. S. Verma, N. J. Walton, G. Grogan, *Acta Crystallogr. D Biol. Crystallogr.* **2006**, *62*, 1494.
[3] A. Maraite, T. Schmidt, M. B. Ansöerge-Schumacher, A. M. Brzozowski, G. Grogan, *Acta Crystallogr. Sect. F* **2007**, *63*, 546.
[4] A. S. Demir, M. Pohl, E. Janzen, M. Müller, *J. Chem. Soc. Perkin. Trans.* **2001**, *7*, 633.
[5] M. Knoll, M. Müeller, J. Pleiss, M. Pohl, *Chembiochem* **2006**, *7*, 1928.
[6] A. S. Demir, H. Hamamci, O. Sesenoglu, F. Aydogan, D. Capanoglu, R. Neslihanoglu, *Tetrahedron: Asymmetry* **2001**, *12*, 1953.
[7] A. van den Wittenboer, B. Niemeijer, S. K. Karmee, M. B. Ansörge-Schumacher, *J. Mol. Catal. B Enzym.* **2010**, *67*, 208.
[8] S. Chakraborty, N. Nemeria, A. Yep, M. J. McLeish, G. L. Kenyon, F. Jordan, *Biochemistry* **2008**, *47*, 3800.
[9] P. Ayhan, A. S. Demir, *Adv. Synth. Catal.* **2011**, *353*, 624.
[10] M. Müller, D. Gocke, M. Pohl, *FEBS. J.* **2009**, *276*, 2894.
[11] G. S. Brandt, N. Nemeria, S. Chakraborty, M. J. McLeish, A. Yep, G. L. Kenyon, G. A. Petsko, F. Jordan, D. Ringe, *Biochemistry* **2008**, *47*, 7734.
[12] T. G. Mosbacher, M. Müeller, G. E. Schulz, *FEBS. J.* **2005**, *272*, 6067.
[13] R. A. W. Frank, A. J. Price, F. D. Northrop, *J. Mol. Biol.* **2007**, *368*, 639.
[14] A. K. Steinbach, S. Fraas, J. Harder, A. Tabbert, H. Brinkmann, A. Meyer, U. Ermler, P. M. Kroneck, *J. Bacteriol.* **2011**, *193*, 6760.
[15] D. Dobritzsch, S. König, G. Schneider, G. Lu, *J. Biol. Chem.* **1998**, *273*, 20196.
[16] A. Dawson, M. J. Chen, P. K. Fyfe, Z. Guo, W. N. Hunter, *J. Mol. Biol.* **2010**, *401*, 253.
[17] A. K. Bera, L. S. Polovnikova, J. Roestamadji, T. S. Widlanski, G. L. Kenyon, M. J. McLeish, M. S. Hasson, *J. Am. Chem. Soc.* **2007**, *129*, 4120.
[18] E. Fullam, F. Pojer, T. Bergfors, T. A. Jones, S. T. Cole, *Open Biol.* **2012**, *2*, 110026.
[19] P. Ayhan, I. Simsek, B. Cifci, A. S. Demir, *Org. Biomol. Chem.* **2011**, *9*, 2602.
[20] P. D. de María, S. Thomas, P. Martina, W. Stefan, D. Karlheinz, G. Harald, T. Harald, L. Andreas, *J. Mol. Catal. B Enzym.* **2006**, *38*, 43.
[21] M. Pohl, B. Lingen, M. Müller, *Chem. Eur. J.* **2002**, *8*, 5288.
[22] A. S. Demir, O. Sesenoglu, E. Eren, B. Hosrik, M. Pohl, E. Janzen, D. Kolter, R. Feldmann, P. Dünkelmann, M. Müller, *Adv. Synth. Catal.* **2002**, *344*, 96.
[23] M. Sanchez-Gonzalez, J. P. N. Rosazza, *Adv. Synth. Catal.* **2003**, *345*, 819.
[24] A. S. Demir, O. Sesenoglu, P. Dünkelmann, M. Müller, *Org. Lett.* **2003**, *5*, 2047.
[25] (a) P. Georgieva, F. Himo, *J. Comput. Chem.* **2010**, *31*, 1707; (b) R. Z. Liao, J. G. Yu, F. Himo, *Inorg. Chem.* **2009**, *48*, 1442; (c) P. Velichkova, F. Himo, *J. Phys. Chem. B* **2005**, *109*, 8216; (d) S. L. Chen, W. H. Fang, F. Himo, *J. Phys. Chem. B* **2007**, *111*, 1253.
[26] L. Yang, R. Z. Liao, J. G. Yu, R. Z. Liu, *J. Phys. Chem. B* **2009**, *113*, 6505.
[27] M. Feliks, G. M. Ullmann, *J. Phys. Chem. B* **2012**, *116*, 7076.
[28] L. J. Zhao, X. Y. Ma, R. G Zhong, *Int. J. Quantum Chem.* **2013**, *113*, 1299.
[29] X. Li, Q. C. Zheng, H. X. Zhang, *Int. J. Quantum Chem.* **2012**, *112*, 619.
[30] J. Y. Wang, H. Dong, S. H. Li, H. W. He, *J. Phys. Chem. B* **2005**, *109*, 18664.
[31] X. Sheng, Y. J. Liu, C. B. Liu, *J. Mol. Graph. Model.* **2013**, *39*, 23.
[32] Q. Q. Hou, J. Gao, Y. J. Liu, *Theor. Chem. Acc.* **2012**, *131*, 1280.
[33] M. W. van der Kamp, A. J. Mulholland, *Biochemistry* **2013**, *52*, 2708.
[34] M. J. Frisch, G. W. Trucks, H. B. Schlegel, G. E. Scuseria, M. A. Robb, J. R. Cheeseman, G. Scalmani, V. Barone, B. Mennucci, G. A. Petersson, H. Nakatsuji, M. Caricato, X. Li, H. P. Hratchian, A. F. Izmaylov, J. Bloino, G. Zheng, J. L. Sonnenberg, M. Hada, M. Ehara, K. Toyota, R. Fukuda, J. Hasegawa, M. Ishida, T. Nakajima, Y. Honda, O. Kitao, H. Nakai, T. Vreven, J. A. Montgomery, Jr., J. E. Peralta, F. Ogliaro, M. Bearpark, J. J. Heyd, E. Brothers, K. N. Kudin, V. N. Staroverov, T. Keith, R. Kobayashi, J. Normand, K. Raghavachari, A. Rendell, J. C. Burant, S. S. Iyengar, J. Tomasi, M. Cossi, N. Rega, J. M. Millam, M. Klene, J. E. Knox, J. B. Cross, V. Bakken, C. Adamo, J. Jaramillo, R. Gomperts, R. E. Stratmann, O. Yazyev, A. J. Austin, R. Cammi, C. Pomelli, J. W. Ochterski, R. L. Martin, K. Morokuma, V. G. Zakrzewski, G. A. Voth, P. Salvador, J. J. Dannenberg, S. Dapprich, A. D. Daniels, O. Farkas, J. B. Foresman, J. V. Ortiz, J. Cioslowski, D. J. Fox, *Gaussian 09*, Gaussian, Inc, Wallingford, CT, **2010**.
[35] G. M. Morris, D. S. Goodsell, R. S. Halliday, R. Huey, W. E. Hart, R. K. Belew, A. J. Olson, *J. Comput. Chem.* **1998**, *19*, 1639.
[36] V. Barone, M. Cossi, J. Tomasi, *J. Comput. Chem.* **1998**, *19*, 404.
[37] J. Tomasi, M. Persico, *Chem. Rev.* **1994**, *94*, 2027.
[38] M. E. S. Lind, F. Himo, *Angew. Chem. Int. Ed.* **2013**, *52*, 4563.
[39] P. E. M. Siegbahn, F. Himo, *WIREs. Comput. Mol. Sci.* **2011**, *1*, 323.
[40] R. Z. Liao, F. Himo, *ACS Catal.* **2011**, *1*, 937.
[41] G. Hübner, K. Tittmann, M. Killenberg-Jabs, J. Schäffner, M. Spinka, H. Neef, D. Kern, G. Kern, G. Schneider, C. Wikner, S. Ghisla, *Biochim. Biophys. Acta* **1998**, *1385*, 221.
[42] A. Bar-Ilan, V. Balan, K. Tittmann, R. Golbik, M. Vyazmensky, G. Hübner, Z. Barak, D. M. Chipman, *Biochemistry* **2001**, *40*, 11946.
[43] E. J. Delgado, J. B. Alderete, G. A. Jana, *J. Mol. Model.* **2011**, *17*, 2735.
[44] R. Friedemann, K. Tittmann, R. Golbik, G. Hübner, *J. Mol. Catal. B* **2009**, *61*, 36.
[45] Y. A. Müller, Y. Lindqvist, W. Furey, G. E. Schulz, F. Jordan, G. Schneider, *Structure* **1993**, *1*, 95.
[46] H. B. Bürgi, J. D. Dunitz, *Acc. Chem. Res.* **1983**, *16*, 153.

Received: 31 July 2013
Revised: 1 October 2013
Accepted: 10 October 2013
Published online 5 November 2013